Available online at www.sciencedirect.com
SCIENCE DIRECT®
Journal of Sound and Vibration 287 (2005) 505–523
JOURNAL OF SOUND AND VIBRATION
www.elsevier.com/locate/jsvi

Determining the response of infinite, one-dimensional, non-uniform periodic structures by substructuring using waveshape coordinates

G.P. Brown*, K.P. Byrne

School of Mechanical and Manufacturing Engineering, The University of New South Wales, Sydney, NSW 2052, Australia

Received 6 February 2004; received in revised form 10 August 2004; accepted 11 November 2004
Available online 3 February 2005

Abstract

A method is presented for determining the wavenumbers, waveshapes and point receptances for an infinite, one-dimensional, non-uniform periodic structure with distributed periodic attachments or supports. The approach is based on a general theory of harmonic wave propagation in one-dimensional periodic systems. Ill-conditioning was previously reported as an impediment to applying the theory to problems of practical importance. In this paper ill-conditioning problems are overcome and a method of substructuring using waveshape coordinates is presented that dramatically improves computational efficiency. The accuracy and generality of the new method are tested by comparing computed and measured receptances for a typical TGV railway track with UIC60 rail, rail pad, ballast and concrete sleepers. The computed results are found to correlate well with measured data.

1. Introduction

A periodic system was defined by Mead [1] as any group of identical elements coupled together in identical ways to form a whole system. A one-dimensional periodic system is one in which the

*Corresponding author. c/o Ford Australia, Proving Ground, Sandy Creek Road, Lara, Vic. 3212, Australia. Tel.: +61 3 5279 6137; fax: +61 3 5282 2672.
E-mail address: gbrow135@ford.com (G.P. Brown).

0022-460X/$ - see front matter © 2004 Elsevier Ltd. All rights reserved.
doi:10.1016/j.jsv.2004.11.015

periodically repeating elements are coupled together end-to-end only [1]. Perhaps, the most obvious example of such a system is a beam with periodic supports or additions.

A uniform periodic structure is one in which the periodic additions can be considered to occur only at the boundaries of the periodically repeating elements. In the case where the beam is augmented with periodic attachments or supports that are not at the periodic boundaries, the system is a non-uniform periodic structure. Examples are shown in Fig. 1.

Solution methods for uniform periodic structures are inherently simpler than for the non-uniform case. Consequently, distributed attachments to periodically repeating elements have often been modelled as if they occur discretely at the periodic element boundaries, rather than in a manner that represents the true attachment length [2–5]. This may be a reasonable idealization when the attached length is short relative to the periodic length and when structural wavelengths are much greater than the attached length. However, if these conditions are not met, such models may be inadequate.

Valuable contributions to the study of periodic structures were made by Mead [1,2,6–9], who was responsible for many advances and insights in this field. In particular, Mead [1] presented the foundation for modelling waves of a general type, not being restricted to uncoupled flexural or longitudinal waves as in previous studies. Mead's method also allowed the periodic elements to be of a non-uniform nature and suggested the suitability of the finite element method as a means of furthering the study of wave propagation in such systems.

Tassilly [10] used a very elegant, classical periodic structure method to explore the behaviour of free flexural waves in a beam with periodically varying mechanical properties. He derived the dispersion relation between wavenumber and frequency for a class of non-uniform periodic elements. Although his model did consider the length of the distributed non-uniformity, the classical beam model that he used did not permit cross-sectional deformation. He also did not provide a means of calculating the forced response of the beam.

Thompson [11] built on the periodic structure theory developed by Mead and used the finite element technique to exploit its advantages. The subject of Thompson's model was a railway track, a common one-dimensional periodic structure. Thompson assumed that the rails act independently and that they are continuously supported. Because of these assumptions he was able to use an arbitrarily short length of rail, a single finite element in length, as the periodic element. This method was extremely efficient as a 10 mm length of rail was able to be used to model a rail that was in fact infinitely long. The periodic element contained no interior coordinates as it was not necessary to account for non-uniformity within the repeating structural element. Elimination of the interior coordinates greatly simplified the numerical problem and using the finite element method, the rail cross-sectional deformation was able to be included for the first time. However, because of the continuous support assumption, the fact that rails are periodically supported by the sleepers was not able to be considered.

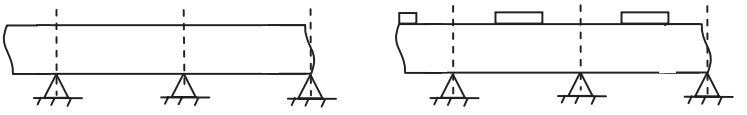

Fig. 1. A comparison of uniform and non-uniform periodic structures.

Gavric [12] used the concepts of cross-section modes and finite elements to calculate the dispersion relation for an infinite, free UIC60 rail. Cross-sectional deformation was represented, but he considered only an infinite uniform structure and did not include a means of calculating the forced response of the rail.

Gry and Gontier [3,4] were also concerned with rail vibrations at acoustic frequencies. They incorporated the important advance made by Thompson, using a finite element approach to include cross-sectional deformation, but they also sought to include the influence of the periodic rail supports. They claimed that problems exist with Mead's periodic structure theory when including internal coordinates. It seems that the presence of evanescent waves with high vibration decay rates may cause the equations of motion to become ill-conditioned and that in the general case the method fails. Gry [3] concluded that there are unsolvable numerical difficulties in the coupling coordinates eigenvalue calculation for all but the most trivial applications of the generalized one-dimensional periodic structure theory.

Having rejected using the periodic structure theory due to numerical problems, Gry [3] proposed an alternative method using transfer matrices and a waveshape basis generated at a single frequency for the infinite rail. He then used this reduced set of coordinates at higher frequencies, eliminating the shapes responsible for the ill-conditioning and attaching the support impedances at discrete points. In a later paper, Gry and Gontier [4] further developed the method using cross-section modes from a finite element model in concert with transfer matrices and Fourier series to avert the need for longitudinal discretization of the rail. Still, no account was made for the distributed nature of the periodic attachment, in this case the rail support.

The method presented in this paper allows analysis of generalized, non-uniform, one-dimensional periodic structures. The length associated with any non-uniformity is fully accounted for and since the finite element method is used, the periodic element may take any form, not being restricted to simple beam models as in the case of classical methods. Complex cross-sectional deformation of beams is therefore permitted. The advantages of this method lie in greater generality and potentially greater accuracy relative to previously reported methods. There is also a significant advantage in terms of computational effort compared with simply implementing a classical periodic structure approach using the finite element method.

Remington [13] has shown that an important quantity in predicting wheel–rail noise due to the rolling of wheels along a railway track is the point receptance of the rail, particularly in the vertical direction and one objective of this paper is to calculate this receptance.

2. Modelling approach

In this paper the freely vibrating waveshapes, propagation constants and driving point receptance are determined for an infinite, one-dimensional, periodic structure, the periodic elements being non-uniform along their length. The approach is first illustrated using a symmetric, non-uniform periodic element consisting of three uniform sub-structures to represent the infinite periodic structure. A new technique which combines the finite element method, periodic structure theory and substructuring using waveshape coordinates is employed. The approach is then applied to a more complicated system, the periodically supported UIC60 rail studied by Gry [3]. The computed receptances are compared with the measured receptance data that he presented.

2.1. Calculation of waveshapes and propagation constants

The first stage in determining the dynamic response of an infinite periodic structure using periodic structure theory is to find the freely vibrating waveshapes and propagation constants for a single periodic element. The waveshapes and propagation constants can then be used in concert with a forcing vector to determine the forced response of the infinite structure.

The key steps in formulating a non-uniform periodic structure problem to find the waveshapes and propagation constants using the approach of Mead [1] are described below.

Each periodic element may be described in terms of the coordinates interior to the element and those at the element boundaries, called the coupling coordinates. Fig. 2 shows, in schematic form, the distinction between different types of coordinates in the non-uniform periodic structure problem.

The displacements and exterior forces at the boundaries of a periodic element are related by a complex propagation constant μ such that:

$$\{q\}_r = \mathrm{e}^{\mu}\{q\}_l \text{ and } \{F\}_r = -\mathrm{e}^{\mu}\{F\}_l. \tag{1}$$

The real part of μ is associated with the decay of a wave between corresponding points on adjacent periodic elements while the imaginary component describes the phase difference between those points.

For an infinite periodic structure there exists a set of characteristic freely vibrating waveshapes $[\Psi]$, which are analogous to the normal modes of vibration in a finite structure. These waveshapes are the unscaled displacement vectors which may be used as a basis to describe the forced response of the periodic structure. The waveshapes involve both cross-sectional deformation and displacements along the infinite axis.

Harmonic motion of a non-uniform periodic element may be described by Eq. (2), which is partitioned so as to identify the left and right coupling coordinates and the interior coordinates as shown in Fig. 2. In the absence of externally applied loads there are no forces applied to the interior of the element and so the interior coordinate force, F_i, is zero.

$$\begin{bmatrix} D_{ll} & D_{li} & D_{lr} \\ D_{il} & D_{ii} & D_{ir} \\ D_{rl} & D_{ri} & D_{rr} \end{bmatrix} \begin{Bmatrix} q_l \\ q_i \\ q_r \end{Bmatrix} = \begin{Bmatrix} F_l \\ 0 \\ F_r \end{Bmatrix}. \tag{2}$$

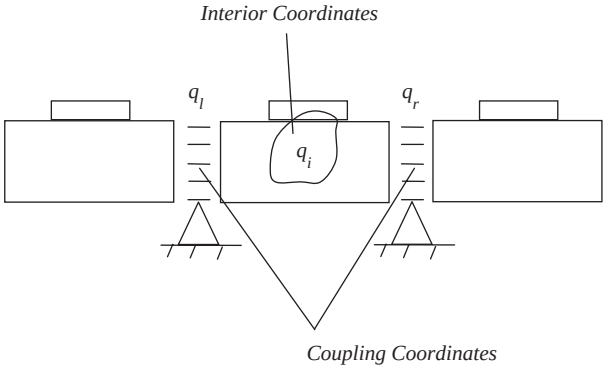

Fig. 2. Schematic diagram showing periodic element coordinates.

The $[D]$ matrix is the dynamic stiffness matrix for the periodic element and is formed from the mass and stiffness matrices such that $[D] = [K] - \omega^2[M]$.

The waveshapes and propagation constants for a periodic element may be found by formulating and solving the coupling coordinates eigenvalue problem for the periodic element by substituting the boundary conditions from Eq. (1) into Eq. (2). In doing this, the coordinates at the right-hand boundary of the periodic element are eliminated to produce Eq. (3):

$$\begin{bmatrix} D_{ll} & D_{li} & D_{lr} \\ D_{il} & D_{ii} & D_{ir} \\ D_{rl} & D_{ri} & D_{rr} \end{bmatrix} \begin{Bmatrix} q_l \\ q_i \\ q_l e^{\mu} \end{Bmatrix} = \begin{Bmatrix} F_l \\ 0 \\ -F_l e^{\mu} \end{Bmatrix}. \tag{3}$$

In the first instance this results in an eigenvalue problem in terms of ω^2. Rearrangement of the problem to make e^{μ} the eigenvalue for known frequency values ω_0 results in the quadratic eigenvalue problem of Eq. (4) as given by Mead [1],

$$\left(e^{\mu} \begin{bmatrix} D_{lr} & 0 \\ D_{ir} & 0 \end{bmatrix} + \begin{bmatrix} D_{ll} + D_{rr} & D_{li} \\ D_{il} & D_{ii} \end{bmatrix} + e^{-\mu} \begin{bmatrix} D_{rl} & D_{ri} \\ 0 & 0 \end{bmatrix} \right) \begin{Bmatrix} q_l \\ q_i \end{Bmatrix} = \begin{Bmatrix} 0 \\ 0 \end{Bmatrix}. \tag{4}$$

In fact, Eq. (4) can be reduced to a simpler form without significant loss of generality where there is more than one cross-section of interior coordinates. This case is very common when using the finite element method and results in the $[D_{lr}]$ and $[D_{rl}]$ partitions being null matrices. After a little manipulation Eq. (4) is reduced to the first-order generalized eigenvalue problem $([A] + \lambda[B])q = 0$ shown in Eq. (5),

$$\left(\begin{bmatrix} D_{ll} + D_{rr} & D_{li} \\ D_{ir} & 0 \end{bmatrix} + e^{\mu} \begin{bmatrix} 0 & D_{ri} \\ D_{il} & D_{ii} \end{bmatrix} \right) \begin{Bmatrix} q_l \\ q_i \end{Bmatrix} = \begin{Bmatrix} 0 \\ 0 \end{Bmatrix}. \tag{5}$$

The solution of Eq. (5) produces vectors of generally complex waveshapes, $[\Psi]$, and the eigenvalues, e^{μ}, from which the complex propagation constants may be found.

Eq. (5) is far simpler than Eq. (4), but the matrices have the same shortcomings as in the earlier formulation. Finding a solution to Eq. (5) is problematic as the matrices are non-symmetric, non-positive definite and subject to singularities. This does not necessarily mean that the solution to the eigenvalue equation is singular or ill-conditioned [14, p. 274], but in order to solve an eigenvalue problem of this type an extremely robust algorithm is required. The QZ algorithm [15,16] is capable of dealing with the generalized eigenvalue problem where the $[A]$ and/or $[B]$ matrices are singular and would seem to be the only way to satisfactorily overcome the numerical difficulties inherent in the present problem.

Unfortunately, the solution to the generalized eigenvalue problem using the QZ algorithm is computationally intensive. The QZ algorithm involves transforming the $[A]$ and $[B]$ matrices to an upper-triangular form, a process for which the solution time is proportional to the cube of the number of degrees of freedom (dof) in the problem.

Mead's method is general and can, in principle, be applied to any periodic structure, for example, a periodically supported rail. However, in the authors' experience the finite element implementation of the method often results in excessive computational cost and there are problems associated with ill-conditioned matrices.

One method of reducing the solution time for the periodic structure model of a beam is to reduce the number of beam cross-sectional coordinates. Instead of reducing the number of physical coordinates, it should be possible, at least in principle, to utilize knowledge of the cross-sectional waveshapes of the beam to formulate the problem using a smaller number of waveshape coordinates. This basic principle has previously been applied by Gry and Gontier [4] for a uniform structure using transfer matrices and by Gavric [12] using a finite element approach. The study described here is the first instance that the authors are aware of that such a method has been applied directly to the dynamic stiffness matrix for a non-uniform periodic element. It is also the first time that such an approach has been used to divide a one-dimensional periodic element into uniform substructures along the periodic length.

2.2. Substructuring using waveshape coordinate reduction

The basis of the method presented in this paper, substructuring using waveshape coordinate reduction, is to divide the non-uniform periodic structure into a number of uniform substructures along the periodic axis and to reduce the number of coordinates in each substructure. The dynamic stiffness matrix for the non-uniform periodic element is then reassembled from the reduced substructure matrices. The coupling coordinates eigenvalue problem may then be evaluated to produce the propagation constants and waveshapes for the infinite, non-uniform periodic structure. A diagram showing the framework of the waveshape coordinate reduction solution scheme is presented in Fig. 3. Note that although the periodic element shown in Fig. 3 is symmetric, no assumption of element symmetry is made in formulating the waveshape coordinate reduction method.

Using the methodology shown in Fig. 3, the coupling coordinates eigenvalue problem is first formulated for a short slice model of each substructure. Since each of the substructures is uniform, the eigenvalue problems need not refer to any interior coordinates. Slice models that are a single finite element long may be used as demonstrated by Thompson [11].

The derivation of the eigenvalue problem for the uniform substructures is the same as previously outlined for the generalized method except without the interior coordinates. The standard equation of harmonic motion for a uniform periodic element with periodic boundary conditions is given in Eq. (6),

$$\begin{bmatrix} D_{ll} & D_{lr} \\ D_{rl} & D_{rr} \end{bmatrix} \begin{Bmatrix} q_l \\ q_l e^{\mu} \end{Bmatrix} = \begin{Bmatrix} F_l \\ -F_l e^{\mu} \end{Bmatrix}. \tag{6}$$

The coupling coordinates eigenvalue problem for the uniform periodic structure as developed by Thompson [11] is shown in Eq. (7),

$$\left(\begin{bmatrix} D_{rl} & D_{rr} \\ 0 & I \end{bmatrix} + e^{\mu} \begin{bmatrix} D_{ll} & D_{lr} \\ -I & 0 \end{bmatrix} \right) \begin{Bmatrix} q_l \\ q_r \end{Bmatrix} = \begin{Bmatrix} 0 \\ 0 \end{Bmatrix}. \tag{7}$$

The solution of Eq. (7) may be carried out swiftly owing to the relatively small number of coordinates involved and the resultant eigenvectors and eigenvalues can be used to reduce the coordinate set for each of the substructures.

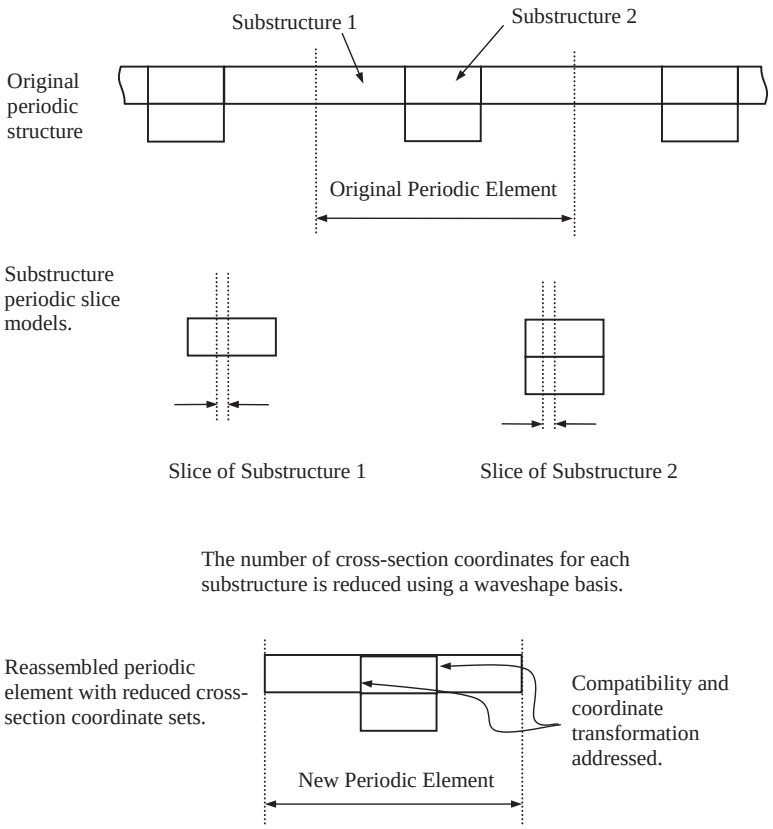

Fig. 3. Framework for coordinate reduction solution scheme.

The second stage of the waveshape coordinate reduction scheme shown in Fig. 3 is to reduce the number of coordinates for each of the substructure cross-sections. For free vibrations it is clear that a reduced modal basis may be substituted for the physical coordinate system, resulting in multiplication of the dynamic stiffness matrix as a whole,

$$\{q\} = [\Psi]\{A\}. \tag{8}$$

{A} contains the generalized coordinates and $[\Psi]$ is the matrix of waveshapes for a complete periodic element.

The waveshape matrix for the complete periodic element, $[\Psi]$, contains not only cross-sectional deformation, but the pattern of structural displacements along the periodic axis. Instead of using a conventional modal substitution, the part of the waveshape that describes the cross-sectional deformation for each uniform substructure, $[\Psi]_{\text{x-sect.}}$, can be used to reduce the number of coordinates on individual structural cross-sections.

After solving the periodic structure problem for a slice of each substructure, one element in length and bounded by two nodal cross-sections, waveshape cross-sectional coordinates are

substituted for the physical coordinate $\{q\}$ on each nodal cross-section of the full model:

$$\{q\}_{\text{x-sect.}} = [\Psi]_{\text{x-sect.}}\{A\}. \tag{9}$$

A reduced cross-sectional waveshape basis is used in Eq. (9). The significant waveshapes to be included in the coordinate substitution may be determined according to their contribution to the driving point receptance of the substructure or simply on the basis of their wavenumber, those with the shortest wavelengths and/or highest vibration decay rates being eliminated from further calculations.

Having established the significant cross-sectional waveshapes for each substructure, the dynamic stiffness matrix $[D]$, for each substructure is partitioned according to the number of physical coordinates on each of the structure cross-sections as shown in Eq. (10).

$$D = \begin{bmatrix} \begin{bmatrix} D_{S11} \end{bmatrix} & \begin{bmatrix} D_{S12} \end{bmatrix} & \cdots & \begin{bmatrix} D_{S1j} \end{bmatrix} \\ \text{x-section 1} & & & \\ \begin{bmatrix} D_{S21} \end{bmatrix} & \begin{bmatrix} D_{S22} \end{bmatrix} & \cdots & \begin{bmatrix} D_{S2j} \end{bmatrix} \\ \text{x-section 2} & & & \\ \vdots & \vdots & \ddots & \vdots \\ \begin{bmatrix} D_{Si1} \end{bmatrix} & \begin{bmatrix} D_{Si2} \end{bmatrix} & \cdots & \begin{bmatrix} D_{Sij} \end{bmatrix} \\ \text{x-section } i & & & \end{bmatrix} \tag{10}$$

The individual $[D]$ matrix partitions are then pre- and post-multiplied by the appropriate subset of waveshape vectors. This has the effect of reducing the number of coordinates on each cross-section of the periodic structure to the number of significant waveshapes. The coordinates belonging to cross-sections at the junctions of the substructures are treated differently to other cross-sectional coordinates. This matter is documented later in the paper.

The reduced dynamic stiffness partitions are generated by a series of matrix multiplications of the form shown in Eq. (11), where the waveshape matrix, $[\Psi]_{\text{x-sect.}}$ is the matrix of cross-sectional shapes from the corresponding uniform substructure,

$$\left[D_{Sij}\right]_{\text{reduced}} = [\Psi]^{\text{T}}_{\text{x-sect.}}\left[D_{Sij}\right][\Psi]_{\text{x-sect.}}. \tag{11}$$

Only the waveshapes belonging to the waves on one of the two axes (either the positive or the negative-going waves) are used in the coordinate reduction.

Once the dynamic stiffness matrices for the substructures have been reduced in dimension using the assumed waveshapes, the periodic element dynamic stiffness matrix is formed by assembling the sub-matrices. The matrix assembly step involves bringing the sets of substructure matrices into a common coordinate system at the junctions of the substructures and ensuring compatibility of forces and displacements at substructure boundaries.

The problem of how to assemble the reduced cross-section substructures is more easily solved than might first be envisaged. The set of physical coordinates at the junction of two substructures provides a common reference system and it is convenient to let the junction coordinates continue to be described in the physical domain. In so doing, the influence of each substructure on the junction dof can be defined by appropriate pre- and/or post-multiplication of the cross-coupling terms in the dynamic stiffness matrix by waveshapes of the corresponding substructure. The special treatment of the matrix partitions surrounding junction cross-sections is shown in Eq. (12). The penalty incurred by not reducing the dof at the junction partitions is likely to be acceptable for periodic elements that have many longitudinal discretizations and few junction cross-sections.

Compatibility of displacements and forces at the junction between the two substructures is automatically satisfied as the terms in the original finite-element-based dynamic stiffness matrix are unaltered at the junction

$$\begin{bmatrix} & \vdots & \vdots & \vdots & \\ \cdots & [\Psi]^{\mathrm{T}}_{\mathrm{x-sect.1}}\left[D_{i-1,j-1}\right][\Psi]_{\mathrm{x-sect.1}} & [\Psi]^{\mathrm{T}}_{\mathrm{x-sect.1}}\left[D_{i-1,j}\right] & [0] & \cdots \\ \cdots & \left[D_{i,j-1}\right][\Psi]_{\mathrm{x-sect.1}} & \left[D_{i,j}\right] & \left[D_{i,j+1}\right][\Psi]_{\mathrm{x-sect.2}} & \cdots \\ \cdots & [0] & [\Psi]^{\mathrm{T}}_{\mathrm{x-sect.2}}\left[D_{i+1,j}\right] & [\Psi]^{\mathrm{T}}_{\mathrm{x-sect.2}}\left[D_{i+1,j+1}\right][\Psi]_{\mathrm{x-sect.2}} & \cdots \\ & \vdots & \vdots & \vdots & \end{bmatrix}.$$

Row of Junction Coordinate Partition

(12)

2.3. Driving point receptance calculation

In order to calculate the driving point receptance for an infinite beam, it is necessary to sort the waveshapes obtained by solving the eigenvalue problem in the previous section into a positive-going wave group and a negative-going wave group. It is therefore of interest to consider the junction of two periodic elements located at the origin as shown in Fig. 4, with the left and right hand side of each element marked LHS and RHS, respectively.

The contributions of the individual waveshapes can be summed to obtain the receptance for a driving point located at the origin as follows:

$$q_j(0) = \sum_{n=1}^{N} A_n \Psi_{jn}, \tag{13}$$

A_n is a vector of participation factors or generalized coordinates.

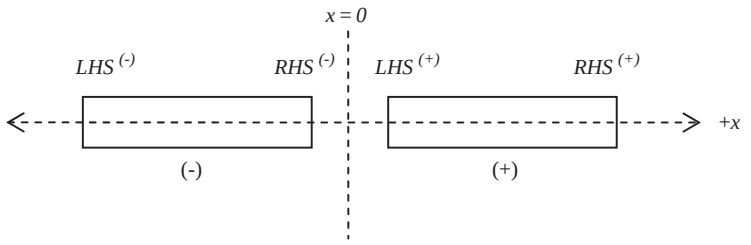

Fig. 4. The junction of two periodic elements at the origin showing the naming and sign convention.

The process of finding the point receptance is achieved by multiplying each unscaled waveshape by the relevant stiffness influence coefficient matrix to determine the relative force contribution of each waveshape displacement. The relative contributions are then scaled such that the total force is unity and the scaled displacement contributions are summed to give the total dynamic displacement for the given force vector.

In order to relate the calculated receptances to the original physical coordinate system it is necessary to transform the response by premultiplying by the slice waveshape matrix as determined in the substructure coordinate reduction. It is also necessary to present the force in the appropriate substructure waveshape coordinate system.

The calculation of the receptance for an infinite, uniform beam using periodic structure theory was described by Thompson [11]. The equations are easily modified to include the interior coordinates. Beginning with the partitioned equations of motion for a single periodic element and making the generalized coordinate substitution given in Eq. (13) leads to expressions for the forces at the left hand end of the positive beam and the right hand end of the negative beam:

$$\begin{bmatrix} D_{ll} & D_{li} & D_{lr} \\ D_{il} & D_{ii} & D_{ir} \\ D_{rl} & D_{ri} & D_{rr} \end{bmatrix} \begin{Bmatrix} q_l \\ q_i \\ q_r \end{Bmatrix} = \begin{Bmatrix} F_l \\ 0 \\ F_r \end{Bmatrix}, \tag{14}$$

$$\{F_l\}^+ = \left([D_{ll}]\left[\Psi_l^+\right] + [D_{li}]\left[\Psi_i^+\right] + [D_{lr}]\left[\Psi_r^+\right]\right)\{A\}, \tag{15}$$

$$\{F_r\}^- = \left([D_{rl}]\left[\Psi_l^-\right]\left[\Psi_r^-\right]^{-1}\left[\Psi_l^+\right] + [D_{ri}]\left[\Psi_i^-\right]\left[\Psi_r^-\right]^{-1}\left[\Psi_l^+\right] + [D_{rr}]\left[\Psi_l^+\right]\right)\{A\}. \tag{16}$$

The total force $\{F\}$ acting at the boundary of the negative and positive axes is the sum of the two forces given in Eqs. (15) and (16) and so:

$$\{F\} = \{F_l\}^+ + \{F_r\}^-. \tag{17}$$

Thompson [11] used a standard matrix inversion routine to find the values of $\{A\}$ for a unit force input involving both the positive- and negative-going waves in the calculation. With the interior coordinates the generalized coordinate, $\{A\}$, can be found from Eq. (18):

$$\{A\} = \begin{pmatrix} [D_{ll}]\left[\Psi_l^+\right] + [D_{li}]\left[\Psi_i^+\right] + [D_{lr}]\left[\Psi_r^+\right] \\ +[D_{rl}]\left[\Psi_l^-\right]\left[\Psi_r^-\right]^{-1}\left[\Psi_l^+\right] + [D_{ri}]\left[\Psi_i^-\right]\left[\Psi_r^-\right]^{-1}\left[\Psi_l^+\right] + [D_{rr}]\left[\Psi_l^+\right] \end{pmatrix}^{-1} \{F\}. \tag{18}$$

The potential for ill-conditioned eigenvalues to be produced in the eigenvalue calculation has to be acknowledged and means that some of the available solutions will, in general, need to be excluded from the receptance calculation. In practice, this means truncating the waveshape basis described in Eq. (13) to include only the well determined eigenvalues. An assessment of eigenvalue quality can be made by reviewing the waveshapes involved to ensure that the finite element mesh is sufficiently refined to represent them and checking that the positive-going eigenvalues are indeed the inverse of the negative-going eigenvalues. This relationship tends to breakdown as the eigenvalues become inaccurate due to a loss of numerical significance.

One limitation of the method shown here is that the receptance cannot be correctly calculated in situations where motion at significant dof is completely eliminated by the periodic attachments. An example of this situation is a beam on perfectly rigid periodic supports. In such cases there are waves that exist within the periodic element that is subject to the external forcing function that cannot be sensed beyond the periodic boundaries. The form of these waves cannot be determined from the coupling coordinates eigenvalue problem [9]. Fortunately, this situation is not a problem in many applications and in the case of the rigid periodic supports, may be overcome by replacing the rigid support with a stiff spring.

3. Application of the model

3.1. The point receptance of an infinite beam of non-uniform cross-section

The method of substructuring using waveshape coordinate reduction for periodic structures is first demonstrated using a simple system, an infinite free beam with periodically attached stiffening in the form of a deeper beam cross-section. Initially, the propagation constants will be found for the structure using Mead's [1] generalized periodic structure theory and then driving point receptances will be calculated for a point on the beam using both the full and reduced periodic element formulation.

Fig. 5 shows the segment of the infinite beam model that constitutes the periodically repeating element in this example. The division of the periodic element into substructures is indicated in the figure and the slice models that will be used to obtain substructure waveshapes are also shown. The parameters relating to the model are shown in Table 1.

Two-dimensional membrane elements having two translational dof at each node have been used to represent the structure. The unstiffened beam cross-section has four physical coordinates, while a cross-section taken through the stiffened substructure has six physical coordinates. The object of this exercise is to show that the number of coordinates can be reduced from four to three on substructure 1 and from six to four on substructure 2 without significant loss of accuracy of the calculated driving point receptance.

The propagation constants for waves on the positive axis for the complete periodic structure model are plotted in Fig. 6. From Fig. 6 it is apparent that there are several attenuation zones between 100 Hz and 5 kHz due to the presence of the periodically attached stiffeners. These are indicated by frequency ranges where the phase is zero or $-\pi$ and the attenuation constant takes on a positive value. There are two independent propagating waves as evidenced by the phase

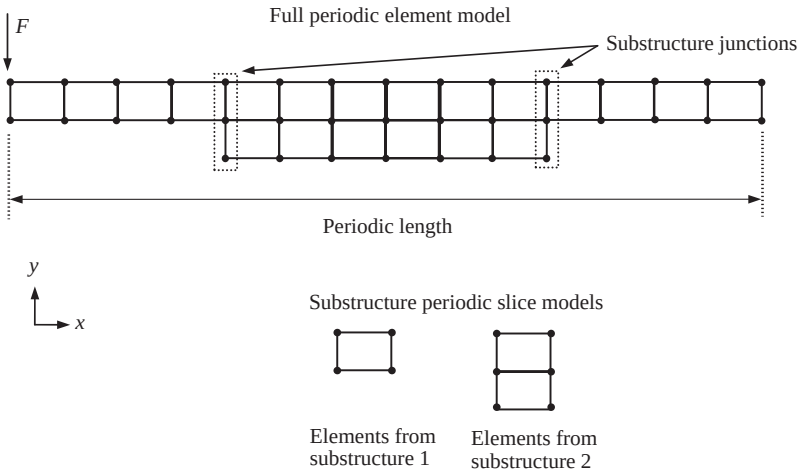

Fig. 5. The periodic element for an infinite beam of non-uniform cross-section.

Table 1
Non-uniform beam model parameters

Periodic length (mm)	350
Element length (mm)	25
E (Pa)	2.1×10^{11}
ν	0.29
ρ (kg/m^3)	8720
η	0.0005
Beam cross-section dimensions	
Substructure 1 (mm)	20×20
Substructure 2 (mm)	20×40

component of the graph and two evanescent or decaying waves indicated in the top segment of the figure.

The driving point receptance for a vertical force located at the point indicated in Fig. 5 is given in Fig. 7 for both the complete and reduced periodic structure models. Fig. 7 shows that the full generalized periodic structure model and the reduced periodic structure model produce near identical driving point receptances for the infinite beam of non-uniform cross-section.

3.2. The point receptance of an infinte periodically supported UIC60 rail

The potency of the coordinate reduction scheme illustrated in the previous trivial example is now demonstrated by applying it to a periodically supported heavy rail. Calculated and experimental results for the driving point receptance at the mid-span of a French TGV railway track were published by Gry [3]. These results are for an infinite UIC60 rail supported by resilient rail pads, bibloc sleepers and ballast. This model represents a significant increase in complexity over the case presented in Section 3.1 as a double layer foundation model is required to

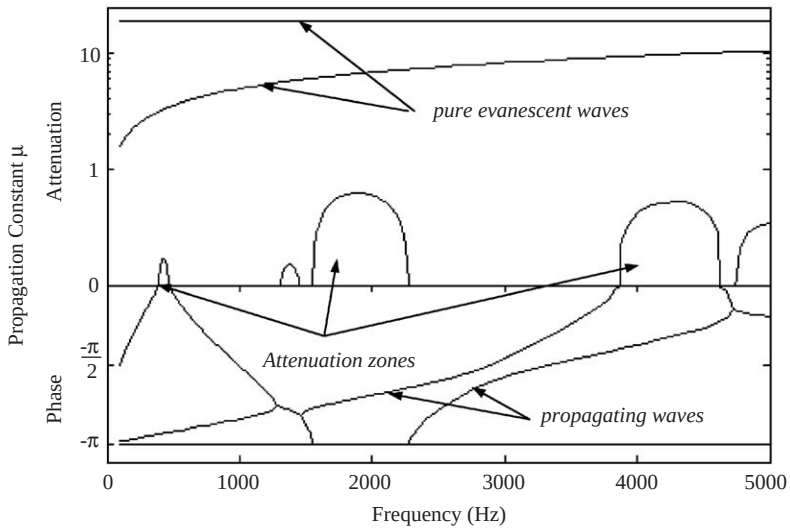

Fig. 6. Propagation constants for positive-going waves on a non-uniform infinite beam.

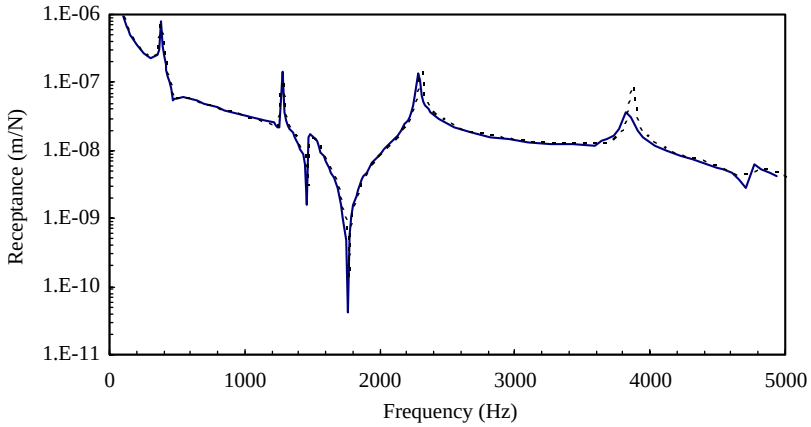

Fig. 7. Vertical driving point receptance for a non-uniform beam: —, full periodic structure model; - - -, reduced periodic structure model (3 coupling coordinates).

characterize the rail support condition. Fig. 8 shows the approximate dimensions of the UIC60 rail section. The properties for the rail, ballast, bibloc sleepers and rail pads as determined by Gry [3] are given in Table 2.

Fig. 9 shows the model of the periodically repeating structure. The rail is modelled by eight-noded linear brick and six-noded wedge elements. The rail pad, sleeper and the ballast are represented as a series of springs and lumped masses. On each supported cross-section the rail pad is represented by three damped translational springs, each with three dof. The base of the rail pad is rigidly connected to the sleeper, which is modelled as an inertial element at the centroid of the sleeper cross-section. The ballast is modelled by a damped six dof spring at the centroid of the

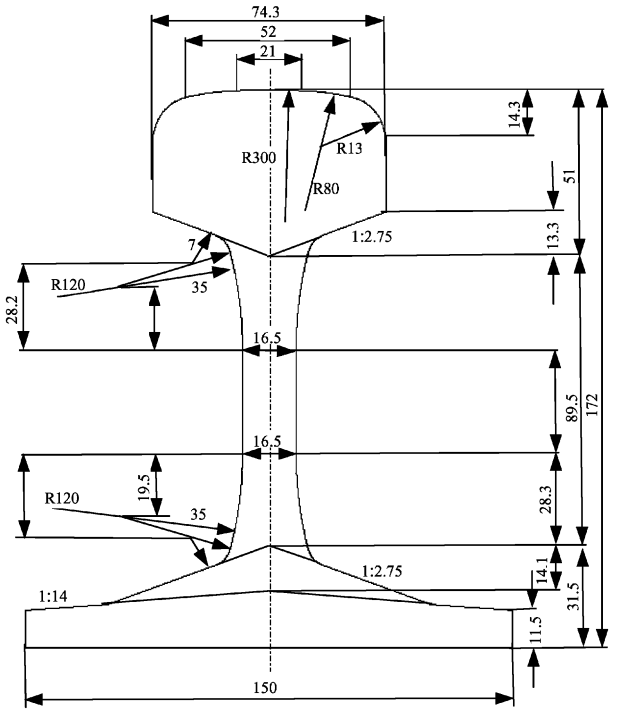

Fig. 8. UIC60 rail dimensions (mm).

Table 2
UIC60 rail model parameters [3]

Rail	E (Pa)	ρ (kg/m^3)		v
	2.1×10^{11}	7850		0.3
		Lateral	Vertical	Longitudinal
Pad	$K_{trans.}$ (N/m)	2.5×10^8	8.5×10^8	5.0×10^8
	η	0.2	0.2	0.2
1/2 Sleeper (m = 122 kg)	I[a] (kg m^2)	0.64	1.32	1.14
Ballast	$K_{trans.}$ (N/m)	3.0×10^8	2.5×10^8	9.5×10^8
	η	0.4	0.4	0.2
	$K_{rot.}$ (N/rad)	2.0×10^8	2.5×10^8	2.0×10^8
	η	0.8	0.8	0.8

[a]Sleeper inertia relative to axes passing through the 1/2 sleeper centroid.

sleeper cross-section. The lumped masses and springs that support the rail at each cross-section have been modelled in a manner consistent with that of Thompson [17] and are independent of foundation elements from adjoining cross-sections. This is a simplifying assumption, preventing wave propagation through the sleeper model.

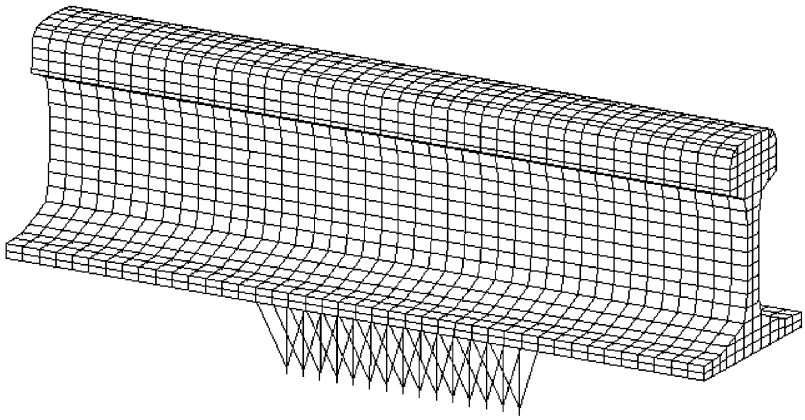

Fig. 9. A periodic structure model of a periodically supported UIC60 rail.

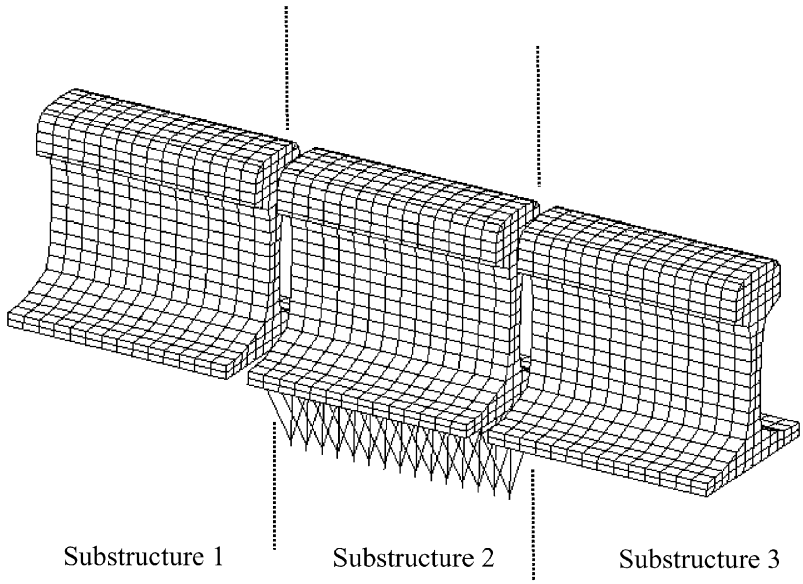

Fig. 10. Substructure models for the periodically supported UIC60 rail.

Substructuring using waveshape coordinate reduction was used to find the receptances for the periodically supported UIC60 rail. The symmetric periodically repeating element was divided into three substructures, a rail segment supported by a distributed sleeper and ballast bounded by two identical unsupported rail segments. The division of the periodic element into substructures is indicated in Fig. 10. The details of the slice models belonging to each substructure are shown in Fig. 11. Substructures 1 and 3 each have 330 coupling coordinates, while substructure 2 has 360 coupling coordinates. A total of only 20 waveshapes were used in the reduced substructure models and in subsequent receptance calculations.

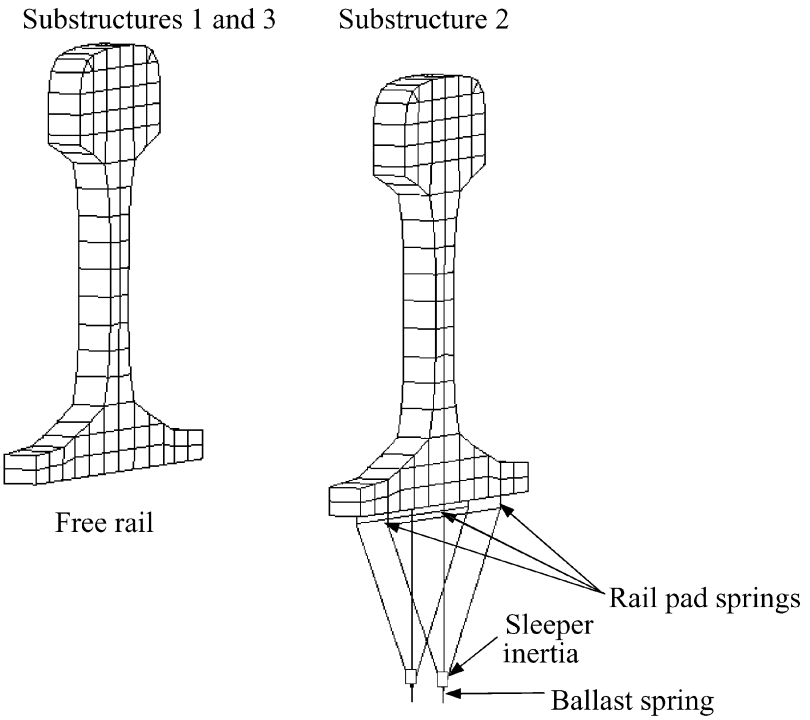

Fig. 11. Substructure slice models for a UIC60 rail.

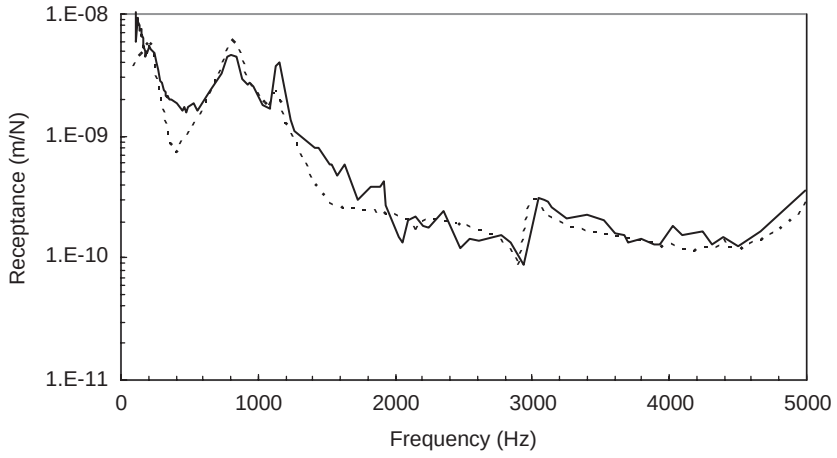

Fig. 12. A comparison of calculated and measured vertical receptances for an infinite periodically supported UIC60 rail: —, measured (Gry); - - - , modelled.

The vertical and lateral driving point receptances were calculated for a point at the top of the rail section at the mid-span of the rail between sleepers to match the data published by Gry [3]. Figs. 12 and 13 show a good correspondence between the calculated and measured receptances

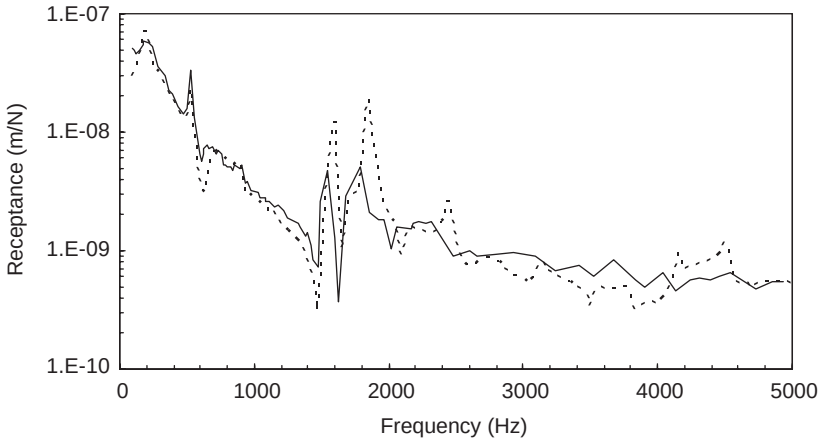

Fig. 13. A comparison of calculated and measured lateral receptances for an infinite periodically supported UIC60 rail: —, measured (Gry); - - - , modelled.

for the infinite periodically supported UIC60 rail for the vertical and lateral directions, respectively.

The example of the UIC60 rail serves to illustrate the potential of the new method to reduce solution times. The advantage over solving the full finite element model of the periodic structure in physical coordinates for the infinite rail with periodic attachments is great. Prior to coordinate reduction using waveshapes, each cross-section of the UIC60 rail model, shown in Fig. 9, had over 300 dof. This number was reduced to 20 on all but the two junction sections using substructuring by waveshape coordinate reduction. The total number of coordinates in the model, including junction coordinates, was reduced from 14,640 to 1540—a reduction by a factor of approximately 10.

Since the QZ method is required to produce reliable solutions to the eigenvalue problem associated with periodic structures and the solution time is proportional to the cube of the number of coordinates, the effect of a 10-fold coordinate reduction in the present case is a reduction in solution time by a factor of about 1000 in comparison to directly implementing Mead's general theory of harmonic wave propagation for periodic structures [1].

4. Conclusions

In this paper a new method has been presented that facilitates the analysis of infinite, non-uniform periodic structures. The method is particularly beneficial in considering structures that have distributed attachments or supports for which no practicable generalized model previously existed.

The results of two test cases have been presented comparing the accuracy of the new method, the method of substructuring using waveshape coordinates, to the method of Mead [1] and to the published experimental data of Gry [3]. There is good agreement between the point receptance calculated using the new method and the application of Mead's theory using finite elements for a simple problem. Similarly, there is good agreement between the results predicted using the new

method and published experimental data for the receptance of a TGV railway track. Together these results show that the numerical limitations of the coupling coordinates eigenvalue calculation found by Gry [3] can be overcome and that Mead's method can be used as a foundation for the accurate calculation of receptances for infinite, non-uniform periodic structures.

Substructuring using waveshape coordinates improves the efficiency of the method of periodic structures for calculating the point receptance of infinite, one-dimensional structures comprising non-uniform periodically repeating elements. An improvement in computational efficiency of a factor of approximately 1000 in comparison to a finite element implementation of Mead's method for general one-dimensional periodic structures has been demonstrated for a problem of practical significance.

Substantial improvements in efficiency together with demonstrated high levels of accuracy mean that the new approach can be used to predict the driving point receptance of a general, non-uniform periodic structure made up of an infinite, uniform, one-dimensional structure with periodically distributed attachments.

Acknowledgement

The authors are grateful to Dr. Arthur Bishop, founder of Bishop Austrans for his generous support of this research.

References

[1] D.J. Mead, A general theory of harmonic wave propagation in linear periodic systems with multiple coupling, *Journal of Sound and Vibration* 27 (1973) 235–260.
[2] D.J. Mead, Free wave propagation in periodically supported infinite beams, *Journal of Sound and Vibration* 11 (1970) 181–197.
[3] L. Gry, Dynamic modelling of railway track based on wave propagation, *Journal of Sound and Vibration* 195 (1996) 477–505.
[4] L. Gry, C. Gontier, Dynamic modelling of railway track: a periodic model based on a generalised beam formulation, *Journal of Sound and Vibration* 199 (1997) 531–558.
[5] M.L. Munjal, M. Heckl, Vibrations of a periodic rail-sleeper system excited by an oscillating stationary transverse force, *Journal of Sound and Vibration* 81 (1982) 491–500.
[6] D.J. Mead, A new method of analysing wave propagation in periodic structures: applications to periodic Timoshenko beams and stiffened plates, *Journal of Sound and Vibration* 104 (1986) 9–27.
[7] D.J. Mead, Wave propagation and natural modes in periodic systems: I mono-coupled systems, *Journal of Sound and Vibration* 40 (1975) 1–18.
[8] D.J. Mead, Wave propagation and natural modes in periodic systems: II multi-coupled systems with and without damping, *Journal of Sound and Vibration* 40 (1975) 19–39.
[9] D.J. Mead, Y. Yaman, The response of infinite periodic beams to point harmonic forces: a flexural wave analysis, *Journal of Sound and Vibration* 144 (1991) 507–530.
[10] E. Tassilly, Propagation of bending waves in a periodic beam, *International Journal of Engineering Science* 25 (1987) 85–95.
[11] D.J. Thompson, Wheel–rail noise generation, part III: rail vibration, *Journal of Sound and Vibration* 161 (1993) 421–426.

[12] L. Gavric, Computation of propagative waves in free rail using a finite element technique, *Journal of Sound and Vibration* 185 (1995) 531–543.
[13] P.J. Remington, Wheel/rail rolling noise, I: theoretical analysis, *Journal of the Acoustical Society of America* 81 (1987) 1805–1823.
[14] G.W. Stewart, J. Sun, *Matrix Perturbation Theory*, Academic Press, San Diego, 1990.
[15] C.B. Moler, G.W. Stewart, An algorithm for generalised matrix eigenvalue problems, *SIAM Journal of Numerical Analysis* 10 (1973) 241–256.
[16] E. Anderson, Z. Bai, C. Bischof, S. Blackford, J. Demmel, J. Dongarra, J. Du Croz, A. Greenbaum, S. Hammarling, A. McKenney, D. Sorensen, 1999. LAPACK User's Guide, third ed. SIAM, Philadelphia, http://www.netlib.org/lapack/lug/lapack_lug.html.
[17] D.J. Thompson, Wheel–Rail Noise: Theoretical Modelling of the Generation of Vibrations, Doctorial Thesis, University of Southampton, 1990.